JOURNAL OF SOLID STATE CHEMISTRY 29, 205–214 (1979)

Magnetic Properties of the Layered Compounds $Ca_2Mn_3O_8$ and $Cd_2Mn_3O_8$*

T. R. WHITE AND W. S. GLAUNSINGER†

Department of Chemistry, Arizona State University, Tempe, Arizona 85281

AND

H. S. HOROWITZ AND J. M. LONGO

Corporate Research Laboratories, Exxon Research and Engineering Company, Linden, New Jersey 07036

Received May 30, 1978; in revised form September 28, 1978

$Ca_2Mn_3O_8$ and $Cd_2Mn_3O_8$, which contain Mn^{4+} monolayers, have been prepared and characterized. Their magnetic susceptibility and electron paramagnetic resonance (EPR) behavior have been examined in detail. The Mn^{4+} moments in both $Ca_2Mn_3O_8$ and $Cd_2Mn_3O_8$ order antiferromagnetically near 60 and 10°K, respectively. Although the Néel temperature in $Ca_2Mn_3O_8$ is in reasonable agreement with molecular-field theory, that in $Cd_2Mn_3O_8$ is well below its expected value. It is proposed that these results, as well as those in the calcium manganite series $CaMnO_3 \rightarrow Ca_2MnO_4$, may reflect the chemical influence of the divalent cation in modifying the Mn–O covalent mixing.

Introduction

Because of the interest in magnetic films, two-dimensional magnetic systems have attracted considerable attention in recent years (*1, 2*). Excellent examples of two-dimensional antiferromagnets are provided by compounds of type A_2MX_4, where A is K or Rb, M is a transitional ion, and X is F or Cl (*3–5*). Although the tetravalent manganese compounds $Ca_4Mn_3O_{10}$, $Ca_3Mn_2O_7$, and Ca_2MnO_4 should provide good examples of magnetic triple-, double-, and monolayer structures, the existing magnetic data for these compounds have been somewhat enigmatic (*6*). To further investigate the magnetic behavior of layered Mn^{4+} compounds, we have undertaken a detailed study of the isostructural compounds $A_2Mn_3O_8$, where A is a divalent cation, and here we report our results for A = Ca or Cd.

The structure of $A_2Mn_3O_8$ is shown in Fig. 1 (*7*). The $Cd_2Mn_3O_8$ analog was first reported by Toussaint (*8*) and subsequently characterized in greater detail by Oswald *et al.* (*9, 10*). The synthesis of $Ca_2Mn_3O_8$ has more recently been published (*11*). In addition, the isostructural Mn_5O_8, where A = Mn^{2+}, has been prepared and characterized (*12*). The structure is monoclinic (space group C_{2h}^3–$C2/m$) and consists of oxygen in the *bc* plane. Between alternate oxygen planes, three-fourths of the possible

* This research was supported in part by a Faculty Research Participation Fellowship (W.S.G.) and Grant DMR 75-09215 from the National Science Foundation.

† To whom inquiries should be addressed.

0022-4596/79/080205-10$02.00/0

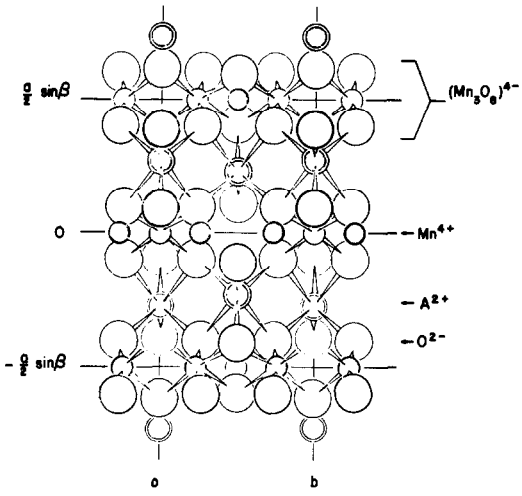

FIG. 1. Structure of $A_2Mn_3O_8$ after Oswald and Wampetich (*10*).

octahedra are occupied to give a layer composition of ($Mn_3O_8^{4-}$). Within these layers, each distorted Mn^{4+} octahedron shares only edges with four other filled Mn^{4+} octahedra. The divalent cations are situated above and below the Mn^{4+} vacancies and serve to hold together the negatively charged $Mn_3O_8^{4-}$ layers. Hence the divalent cations form strongly undulated layers between the $Mn_3O_8^{4-}$ layers. The six oxygen ions surrounding each divalent cation form a trigonal prism, with the cation closer to the three oxygen ions adjacent to the Mn^{4+} vacancy. Since the $Mn_3O_8^{4-}$ layers are separated by undulating A^{2+} layers, the magnetic behavior of these compounds is expected to approximate that of magnetic Mn^{4+} monolayers.

Experimental

Sample Preparation and Characterization

Samples of $Ca_2Mn_3O_8$ and $Cd_2Mn_3O_8$ were prepared from solid-solution calcite precursors (*11, 13*). The precursors were synthesized by first preparing an aqueous solution containing the appropriate molar amounts of A (where A = Ca or Cd) and manganese cations. This aqueous solution was obtained by dissolving ACO_3 and $MnCO_3$ in dilute nitric acid. The ACO_3 used was reagent grade. The $MnCO_3$ used was freshly precipitated from a manganese nitrate solution with large excesses of ammonium carbonate, dried at 100°C in a vacuum oven, and stored in sealed containers until used. Commercially available reagent-grade $MnCO_3$ was unacceptable because it always contained significant amounts of oxidized manganese products, as evidenced by its brown color. The aqueous solution of A and manganese cations was then added, with stirring, to a large excess of approximately 2 M ammonium carbonate. The resulting precipitate was a single-phase, solid-solution carbonate with the calcite structure whose composition could be expressed as $A_2Mn_3(CO_3)_5$. Precipitates were dried at 100°C in a vacuum oven and stored in an inert atmosphere to prevent any premature oxidation of divalent manganese.

The solid solution precursors were reacted to the mixed-metal oxide by firing them in recrystallized alumina boats in an atmosphere of flowing oxygen. $Ca_2Mn_3O_8$ was synthesized by firing its carbonate precursor for 2 hr at 650°C with two interruptions for grinding. $Cd_2Mn_3O_8$ was synthesized by firing its carbonate precursor for 21 hr at 700°C with two interruptions for grinding.

The reacted mixed-metal oxides were examined by powder X-ray diffraction using a Phillips diffracted-beam monochromator.

In order to determine the cation stoichiometry of $Ca_2Mn_3O_8$, this phase was first reduced for about 2 hr in hydrogen at 1000°C. The cubic unit-cell parameter of the resulting single-phase, solid-solution rock salt was refined to ±0.001 Å using eight slow-scanned (0.25°/min) reflections from the 2θ interval of 50–130°. The refinement

was done by computer minimization of the differences between observed and calculated values of 2θ using the Simplex method. Since the unit-cell parameter in the Ca–Mn–O solid-solution system varies linearly with composition (*14*), it was possible to determine the atomic percentage of calcium and manganese present, respectively, to ±0.3%. It was not possible to determine the cation stoichiometry of $Cd_2Mn_3O_8$ using the above method, because reaction conditions that were appropriate for the formation of Mn^{2+} were sufficiently reducing that cadmium metal was also produced. Thus, it was not possible to reduce $Cd_2Mn_3O_8$ to a single-phase rock salt.

Oxygen contents of both phases were established using a Fisher thermogravimetric analyzer containing a Cahn electrobalance. The $Ca_2Mn_3O_8$ was reduced in hydrogen and weight loss was attributed to manganese with oxidation states higher than 2+. The $Cd_2Mn_3O_8$ was reacted with oxygen to form $CdMn_2O_4 + CdO$ and the weight loss was attributed to manganese with oxidation states higher than 3+.

Unit-cell dimensions of $Ca_2Mn_3O_8$ were determined by least-squares refinement of powder diffractometer tracings. Using starting parameters based on the structurally related $Cd_2Mn_3O_8$ (*10*), 71 powder intensities representing 131 reflections were used to refine three atomic temperature factors and 10 positional parameters for Ca, Mn, and O with a Simplex program.

The electrical resistivities of the $A_2Mn_3O_8$ materials were measured on pressed-powder samples by the four-probe method at room temperature. The resistivity cell consisted of a cylindrical die, which allowed pressure to be applied to the sample. The current flow was supplied through the end plungers of the die, while the voltage measurement was made between annular electrodes formed by two metal foils situated between the end plungers. Pressure was applied until the sample's resistivity did not change.

Magnetic Susceptibility Measurements

The magnetic susceptibility was measured in the range 1.5–300°K in a Faraday apparatus described elsewhere (*15*). The maximum field was 13 kG, with $H(dH/dz) = 27\ (kG)^2/cm$. The apparatus was calibrated with platinum and $HgCo(SCN)_4$. At each temperature the susceptibility was determined at five field strengths ranging from 2.5 to 13 kG. For both compounds the susceptibility was independent of the magnetic field strength, and the measured susceptibilities were averaged to obtain the reported values. The susceptibilities have been corrected for ionic diamagnetism and are believed to be accurate within 2%. Independent determinations on two different preparations of each compound were in excellent agreement.

EPR Measurements

Ambient-temperature EPR spectra were recorded on a Varian E-12 spectrometer. Spectra between 77 and 600°K were taken using an X-band reflection spectrometer described elsewhere (*16*). A calibrated, adjustable single-crystal ruby standard positioned near the sample in the microwave cavity was used as an intensity standard and to calibrate large field sweeps. Accurate g-factors were measured using diphenylpicrylhydrazyl and pitch in KCl as internal standards.

Results

The $Cd_2Mn_3O_8$ prepared in this study gave an X-ray diffraction pattern which agreed with that of Oswald *et al.* (*9, 10*) and was judged, on the basis of X-ray diffraction, to be pure. Thermogravimetric reaction with oxygen gave a formula of $Cd_2Mn_3O_{7.9\pm0.1}$ assuming a Cd/Mn ratio of 2/3. The resistivity of pressed-powder samples of this compound was $10^5\ \Omega$-cm. A detailed crystallographic structure refinement from high-resolution X-ray powder data is reported in Ref. (*10*).

The synthesis of pure $Cd_2Mn_3O_8$ is complicated because there appears to be appreciable solid solution between it and the isotypic Mn_5O_8. That is, Cd^{2+} can be replaced by Mn^{2+}, and an insufficiently long reaction time will convert a Cd/Mn (2/3) calcite precursor into a two-phase mixture of $Cd_{2-x}Mn_x^{2+}Mn_3^{4+}O_8 + xCdO$. Thus, one must carefully monitor the progress of the synthesis reaction to ensure that any second-phase CdO has completely reacted. One must also take care that precursor compositions which are manganese-rich [relative to Cd/Mn (2/3)] are not employed, since compositional deviations of this type are detected only as subtle changes in unit-cell dimensions accompanying the substitution of Cd^{2+} by Mn^{2+}.

The $Ca_2Mn_3O_8$ that was prepared gave an experimentally determined cation stoichiometry of 40.66% Ca, 59.34% Mn as compared to a calculated stoichiometry of 40.0% Ca, 60.0% Mn. Thermogravimetric reduction in hydrogen gave a formula of $Ca_2Mn_3O_{8.0\pm0.1}$, assuming a Ca/Mn ratio of 2/3. The synthesis of $Ca_2Mn_3O_8$ is straightforward, and there is no evidence for any substitution of Ca^{2+} by Mn^{2+}.

The structure of $Ca_2Mn_3O_8$ is monoclinic and isostructural with $Cd_2Mn_3O_8$ and Mn_5O_8. The unit-cell dimensions for each of these compounds are listed in Table I. Initial refinement of atomic position and isotropic temperature parameters for $Ca_2Mn_3O_8$ (obtained with the Simplex program) gave an R value ($\Sigma w \Delta I/\Sigma wI$) of 0.032. The details of the refinement and the crystal structure will be reported elsewhere. The measured resistivity of pressed-powder samples of $Ca_2Mn_3O_8$ was 10^5 Ω-cm.

The reciprocal susceptibility per mole of Mn^{4+} for $Ca_2Mn_3O_8$ is plotted as a function of temperature in Fig. 2. The susceptibility obeys the Curie–Weiss law above about 150°K and exhibits a broad maximum at 74 ± 4°K and a minimum near 15°K. The origin of the increase in susceptibility below 15°K is uncertain, but may be due to the sample, impurities, or perhaps a parasitic magnetization. Assuming that the origin of the increase is another Mn^{4+} impurity salt, the estimated amount of impurity present is only 2 mole% Mn^{4+}, which would affect the susceptibility data above 100°K by less than 5%.

The temperature dependence of the reciprocal susceptibility per mole of Mn^{4+} for $Cd_2Mn_3O_8$ is shown in Fig. 3. The Curie–Weiss law is obeyed above about 60°K, and the susceptibility shows a weak maximum near 20 ± 4°K.

The magnetic parameters for these compounds are summarized in Table II. Since only powder susceptibilities have been measured, the Néel temperature (T_N) cannot be accurately determined from the data. T_N can be estimated from the maximum in the susceptibility vs temperature curve, $T(\chi_{max})$;

TABLE I

UNIT-CELL DIMENSIONS OF $A_2Mn_3O_8$ COMPOUNDS[a]

Composition	a (Å)	b (Å)	c (Å)	β (deg)	Mn^{4+} layer separation (Å)
$Ca_2Mn_3O_8$	11.020	5.848	4.942	109.80	5.18
$Cd_2Mn_3O_8$	10.806	5.808	4.932	109.53	5.09
Mn_5O_8	10.347	5.724	4.852	109.25	4.88

[a] The standard deviation of the unit-cell dimensions is ±1 in the last digit.

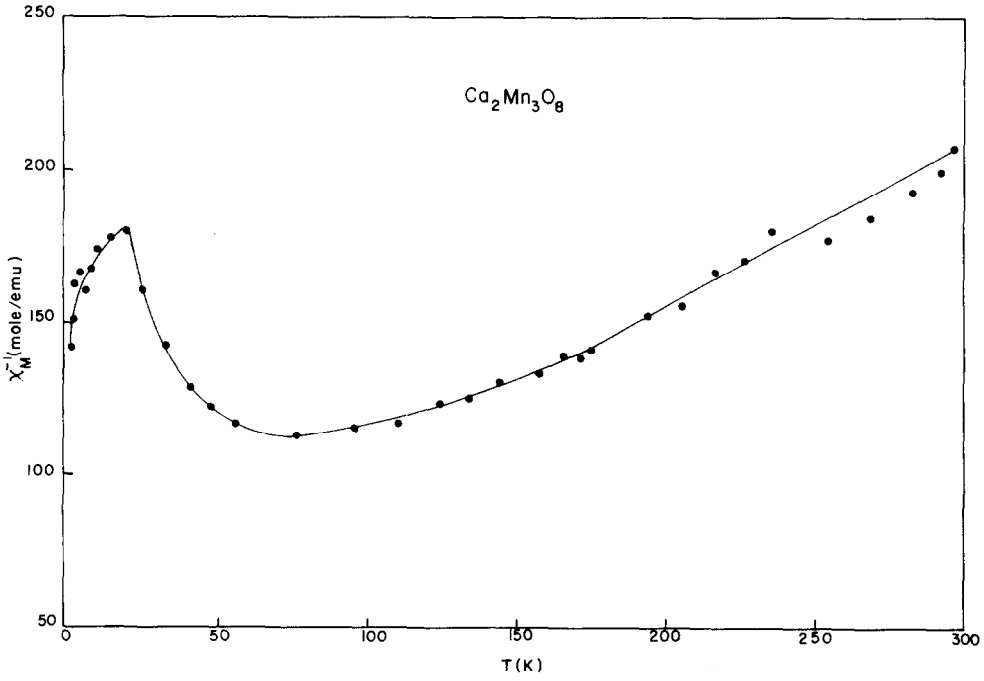

FIG. 2. Reciprocal susceptibility per mole of Mn^{4+} for $Ca_2Mn_3O_8$ as a function of temperature.

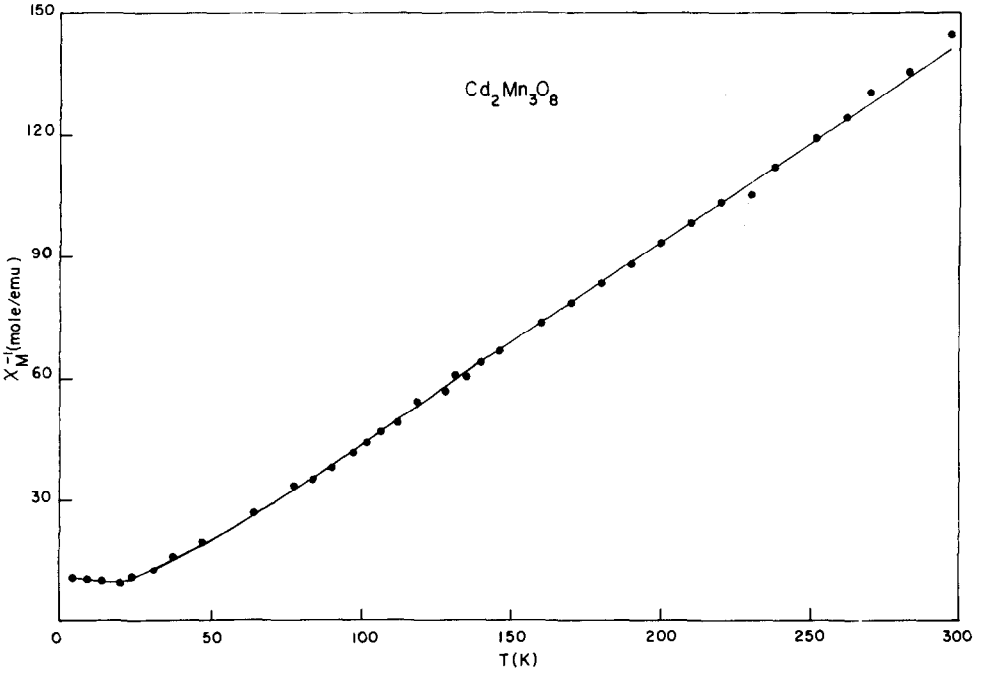

FIG. 3. Reciprocal susceptibility per mole of Mn^{4+} versus temperature for $Cd_2Mn_3O_8$.

TABLE II

MAGNETIC PARAMETERS[a]

Compound	μ_{so} (μ_B)	μ (μ_B)	θ (°K)	T (χ_{max})
$Ca_2Mn_3O_8$	3.87	3.94	−100	74
$Cd_2Mn_3O_8$	3.87	4.01	12	20

[a] μ_{so} and μ are the calculated spin-only and experimental magnetic moments, respectively, in units of the Bohr magneton, and θ is the Weiss constant.

however, the actual T_N may be slightly lower than the temperature at which the susceptibility is a maximum, since there is evidence that the maximum susceptibility occurs at a temperature which is somewhat higher than that at which long-range order occurs (*17–20*).

EPR spectra of $Ca_2Mn_3O_8$ and $Cd_2Mn_3O_8$ at ambient temperature are shown in Fig. 4. The lineshape in each compound is independent of temperature and Lorentzian. Figure 5 displays the temperature dependence of the peak-to-peak linewidth. For $Ca_2Mn_3O_8$, the linewidth is independent of temperature above about 300°K, but below 300°K the linewidth increases with decreasing temperature and approaches a vertical asymptote at 60 ± 5°K. For $Cd_2Mn_3O_8$, line broadening occurs below about 60°K, and the linewidth approaches a vertical asymptote at 10 ± 2°K. The temperature dependence of the integrated intensity of the EPR absorption, although subject to considerable error, is in good agreement with the susceptibility results. Mn^{2+} was not detected, even at the highest spectrometer sensitivities, which indicates the absence of weakly interacting Mn^{2+} in our samples. The EPR parameters, determined from multiple scans at each temperature for both compounds, are given in Table III.

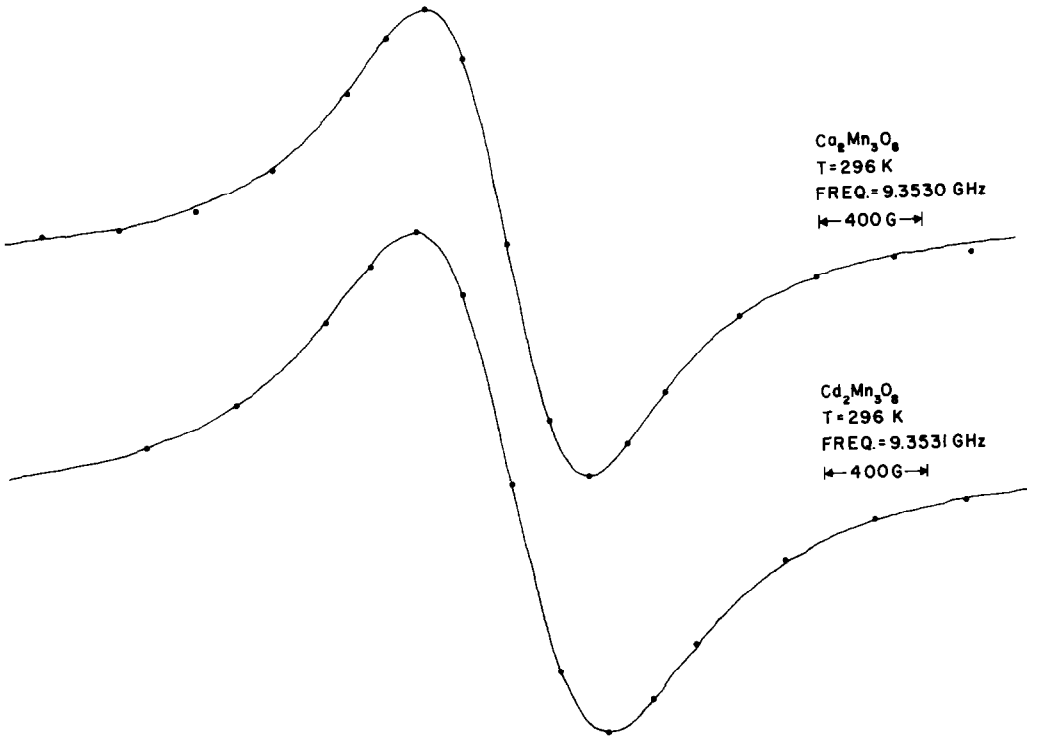

FIG. 4. EPR spectra of $Ca_2Mn_3O_8$ and $Cd_3Mn_2O_8$ at 296°K. The dots are values computed from a Lorentzian lineshape function.

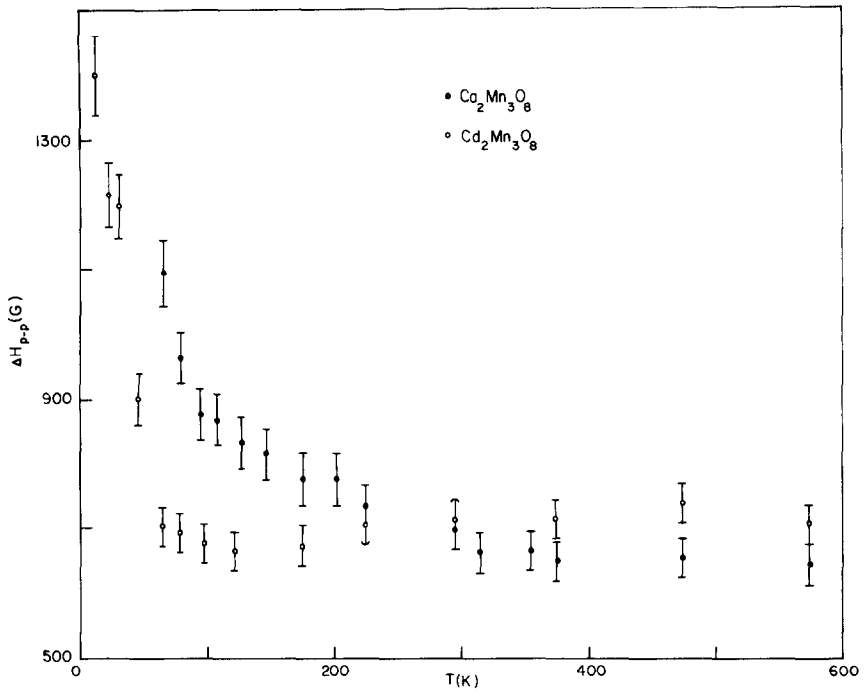

FIG. 5. Temperature dependence of the peak-to-peak linewidth for $Ca_2Mn_3O_8$ and $Cd_2Mn_3O_8$.

EPR spectra for $CaMnO_3$ and Ca_2MnO_4 were also recorded, and their lineshapes were again independent of temperature and Lorentzian. For $CaMnO_3$, where $T_N = 123°K$ (*6*), the linewidth is independent of temperature and equal to 1640 ± 80 G, and the integrated intensity decreases by about an order of magnitude near 123°K. For Ca_2MnO_4, where $T_N = 110°K$ (*21*), the linewidth is independent of temperature above 150°K and equal to about 605 ± 10 G, but below 150°K the linewidth broadens with decreasing temperature and approaches a vertical asymptote near 113°K.

Discussion

The chemical, magnetic susceptibility, and EPR data all show that Mn^{4+} is the dominant paramagnetic species present in these compounds. The close agreement between the spin-only magnetic moment for Mn^{4+} and the experimental moments (Table II) and the proximity of the g-factor to the

TABLE III

EPR PARAMETERS

Compound	ΔH_{p-p}[a] (G)	g	θ (°K)	$T_{\Delta H \to \infty}$ (°K)
$Ca_2Mn_3O_8$	640 ± 30	1.979 ± 0.004	-119 ± 35	60 ± 5
$Cd_2Mn_3O_8$	700 ± 30	1.982 ± 0.004	0 ± 15	10 ± 2

[a] Linewidth at 296°K.

spin-only value indicate that the electronic ground state of Mn^{4+} is the orbital-singlet state $^4A_2$ having a magnetic moment of $3.87\mu_B$. For Mn^{4+} in an axially distorted octahedral environment $g = g_s - 8\lambda/\Delta$ (*22*), where λ is the spin–orbit coupling constant and Δ is the ligand–field splitting. Taking $\lambda = 134\ cm^{-1}$ (*22*), for both compounds we estimate that $\Delta \sim 50{,}000\ cm^{-1}$, which should be an upper limit to Δ since covalency effects have been neglected.

The temperature dependence of the EPR linewidth is in good agreement with the susceptibility data. In general, we expect a vertical asymptote in the linewidth vs temperature plot at T_N and line broadening to begin at temperatures ranging from two to five times T_N (*23*). Hence we have $T_N = 60 \pm 5°K$ for $Ca_2Mn_3O_8$ and $T_N = 10 \pm 2°K$ for $Cd_2Mn_3O_8$, which are both somewhat below $T(\chi_{max})$, as expected. The EPR results for $CaMnO_3$ and Ca_2MnO_4 are in reasonable agreement with a previous study (*6*), except that we observed no line broadening for $CaMnO_3$ near T_N.

We now seek an explanation of the Néel temperatures in $Ca_2Mn_3O_8$ and $Cd_2Mn_3O_8$ and their large discrepancy. In the simple molecular-field approximation, the Néel temperature for antiferromagnetic ordering of two magnetic sublattices having only intersublattice exchange interactions is given by

$$kT_N = -2ZJS(S+1)/3, \qquad (1)$$

where Z is the number of nearest-neighbor magnetic ions having spin S and J is the exchange integral (*24*). Hence T_N for a magnetic monolayer having $Z = 4$ should be two-thirds that for a three-dimensional magnetic structure having $Z = 6$. On the basis of the structure of $A_2Mn_3O_8$, one naively expects their Néel temperatures to be nearly equal and about two-thirds that of their three-dimensional counterpart. From the Néel temperatures for the three-dimensional Mn arrangements in the perovskite-like $CaMnO_3$ ($T_N = 123°K$) (*6*) and monoclinic Mn_5O_8 ($T_N = 136°K$) (*25*), we predict that T_N for $Ca_2Mn_3O_8$ and $Cd_2Mn_3O_8$ may lie in the range 63–82°K. T_N for $Ca_2Mn_3O_8$ is in reasonable agreement with this prediction, and in the molecular-field approximation this suggests that the coefficients describing the sublattice interactions are all small with the exception of the ones describing the nearest-neighbor interactions within a Mn^{4+} layer. However, T_N for $Cd_2Mn_3O_8$ is well below its expected value. This is contrary to what one would predict on the basis of the Mn–Mn distances, since these distances are all larger in $Ca_2Mn_3O_8$ (Table I). A plausible explanation of this behavior involves cation competition for covalent mixing with oxygen (*24*). In the $A_2Mn_3O_8$ structure the Mn^{4+} ions probably interact with each other via an exchange mechanism involving overlap of their t_{2g} orbitals with oxygen $p\pi$ orbitals. However, the oxygen concurrently σ-bonds with the divalent cation. Generally, one anticipates that the more basic, larger cations will result in a larger intralayer Mn–O covalent mixing and hence a greater exchange interaction and a larger T_N. In particular, since Ca is considerably more basic than Cd, we expect, in agreement with experiment, that $T_N(Ca_2Mn_3O_8) > T_N(Cd_2Mn_3O_8)$. That this chemical influence can be so significant is quite reasonable, and indeed similar behavior has been observed in the potassium nickel fluorides $KNiF_3$ and K_2NiF_4 (*19*) and the calcium manganite series $CaMnO_3 \rightarrow Ca_2MnO_4$ (*6*). The interesting result that the Mn^{4+} exchange interactions increase markedly in going from the three-dimensional Mn^{4+} arrangement in $CaMnO_3$ to Mn^{4+} monolayers in Ca_2MnO_4 (*6*) is in accord with the above explanation, since the Mn–O covalent mixing, and hence J, should increase as the Ca/Mn ratio increases. However, it should be pointed out that differences in interionic separation and electrical resistivity in the calcium manganite series (*6*) may also influence their

TABLE IV

MAGNETIC PARAMETERS AND EXCHANGE INTEGRALS

Compound	T_N (°K)	T (χ_{max})	θ (°K)	J/k[a] (°K)
$CaMnO_3$	123[b]			−11.1
Ca_2MnO_4	114[b]	220[b]		−28
$Ca_2Mn_3O_8$	60	74	−100	−9.4
$Cd_2Mn_3O_8$	10	20	12	+1

[a] The values of J given for Ca_2MnO_4, $Ca_2Mn_3O_8$, and $Cd_2Mn_3O_8$ are the intralayer exchange integrals.
[b] Ref. (*6*).

magnetic properties. The lower T_N in $Ca_2Mn_3O_8$ may be due in part to its lower Ca/Mn ratio and considerably smaller Mn–O–Mn bond angle (*26*), which averages to 109.6° in Mn_5O_8 (*7*), than in the perovskite-related calcium manganite series, in which there is maximal 180° superexchange between manganese neighbors.

Further insight into the magnetic behavior of these compounds can be obtained by estimating exchange integrals from the magnetic data. The relevant data and results of our calculations are displayed in Table IV. For $CaMnO_3$, J was determined from T_N using the result of Rushbrook and Wood for a simple-cubic antiferromagnet (*27, 28*):

$$\alpha = 100(\theta_c' - \theta_c)/\theta_c, \qquad (2)$$

where α is a constant for a given S, $\theta_c' = kT_N/J$, and $\theta_c = 5(Z-1)[11\,S(S+1)-1]/384$. Setting $Z=6$, $S=3/2$, and $\alpha = 2.9$, we find $J/k = -11.1°K$. For Ca_2MnO_4 and $Ca_2Mn_3O_8$, the intralayer exchange integral was estimated from T (χ_{max}) using the method of de Jongh (*2, 29*). In addition, the theoretical Weiss constant θ_{th} ($=-T_N$) can be calculated from J using Eq. (1). For $Ca_2Mn_3O_8$, taking $Z=4$ we obtain $\theta_{th} = -94°K$, which is in reasonable agreement with the experimental θ. For $Cd_2Mn_3O_8$, the positive θ coupled with the observed antiferromagnetic ordering suggests that the intralayer exchange interactions are ferromagnetic and that the interlayer exchange interactions are antiferromagnetic and only slightly smaller. Using Eq. (1) and the experimental θ for $Cd_2Mn_3O_8$, we estimate the intralayer exchange integral to be +1°K. A rough estimate of the antiferromagnetic interlayer exchange integral J_{af} can be obtained from the molecular-field result (*30*).

$$\chi_{max} = N_0 g^2 \mu_B{}^2/4Z_{af}|J_{af}|. \qquad (3)$$

Using Eq. (3), we find $Z_{af}|J_{af}|/k \approx 3.4°K$, which is indeed slightly smaller than the ferromagnetic intralayer exchange $Z\,J/K \approx 4°K$. Hence the magnitudes of the intralayer exchange interactions increase in the following manner: $Ca_2MnO_4 \gg CaMnO_3 > Ca_2Mn_3O_8 \gg Cd_2Mn_3O_8$, and possible explanations of this behavior have been given in the previous paragraph.

Finally, we comment upon the width of the EPR lines in these manganite compounds. The Lorentzian lineshape is characteristic of exchange-coupled localized moments (*16*). Since the calculated dipolar width is about 5 kG, the narrow resonances observed indicate extreme exchange narrowing of the Mn^{4+} resonance. For two-dimensional exchange narrowing above the temperature range where critical spin fluctuations occur, the half-width at half-maximum absorption is given by

$$\Delta H = \frac{M_2}{H_e} \ln \frac{H_e}{M_2^{1/2}}, \qquad (4)$$

where H_e is the exchange field and M_2 is the second moment (*31*). Calculating $\Delta H \sim 600$ G and $M_2 \sim 3$ kG^2, we find $H_e \sim 3.5$ kG, so that $T_N \sim 0.5$°K. Hence the predicted exchange fields are about two orders of magnitude too small, which suggests that the ΔH used above is much larger than the true exchange-narrowed linewidth. We estimate that the peak-to-peak linewidth should be about 70 G in $Ca_2Mn_3O_8$ and 190 G in $Cd_2Mn_3O_8$ to obtain the experimental Néel temperatures. Since the linewidth decreases with layer separation, it is tempting to attribute the excess width to dipolar interactions between one magnetic monolayer and the adjacent monolayer to which it is weakly exchange coupled; however, at high temperatures rapid spin fluctuations should average dipolar interactions between monolayers to zero. Since we have estimated that the hyperfine and crystal-field contributions to the second moment make a negligible contribution to the linewidth, at this time we are unable to offer an explanation of the origin of the excess high-temperature linewidth in these compounds, as well as in $CaMnO_3$ and Ca_2MnO_4.

Acknowledgments

The authors wish to acknowledge the assistance of Mr. Alex Chang for measuring the magnetic susceptibility of $Cd_2Mn_3O_8$, Mr. Harold Brady for sample preparation, and Professor M. J. Sienko for permitting us to make the magnetic susceptibility measurements in his laboratory.

We are also grateful to Dr. Gerald Ansell for obtaining the preliminary structure-refinement data for $Ca_2Mn_3O_8$ that have been reported here.

References

1. R. F. SOOKOV, "Magnetic Thin Films," Harper & Row, New York (1965).
2. L. J. DE JONGH AND A. R. MIEDEMA, *Advan. Phys.* **23**, 1 (1974).
3. D. J. BREED, Thesis, University of Amsterdam (1969).
4. R. J. BIRGENEAU, H. J. GUGGENHEIM, AND A. SHIRANE, *Phys. Rev. B* **1**, 2211 (1970).
5. H. W. DE WIJN, L. R. WALKER, AND R. E. WALSTEDT, *Phys. Rev. B* **8**, 285 (1973).
6. J. B. MACCHESNEY, H. J. WILLIAMS, J. F. POTTER, AND R. C. SHERWOOD, *Phys. Rev.* **164**, 779 (1967).
7. H. R. OSWALD AND M. J. WAMPETICH, *Helv. Chim. Acta* **50**, 2023 (1967).
8. H. TOUSSAINT, *Rev. Chim. Miner.* **1**, 141 (1964).
9. H. R. OSWALD, W. FEITKNECHT, AND M. J. WAMPETICH, *Nature* **207**, 72 (1963).
10. H. R. OSWALD AND M. J. WAMPETICH, *Helv. Chim. Acta* **50**, No. 7, 2023 (1967).
11. H. S. HOROWITZ AND J. M. LONGO, *Mater. Res. Bull.*, in press.
12. N. YAMAMOTO, M. KIYAMA, AND T. TAKADA, *Japan. J. Appl. Phys.* **12**, 1827 (1973).
13. L. R. CLAVENNA, J. M. LONGO, AND H. S. HOROWITZ, U.S. Patent 4,060,500 to Exxon Research and Engineering Company (November 29, 1977).
14. A. H. JAY AND K. W. ANDREWS, *J. Iron Steel Inst.* **152**, 15 (1946).
15. J. E. YOUNG, JR., Thesis, Cornell University (1970).
16. W. S. GLAUNSINGER, *J. Magn. Reson.* **18**, 265 (1975).
17. M. F. SYKES AND M. E. FISHER, *Phil. Mag.* **7**, 1731 (1962).
18. M. E. FISHER, *Physica* **28**, 919 (1962).
19. M. E. LINES, *Phys. Rev.* **164**, 736 (1967).
20. R. NAVARRO, J. J. SMIT, L. J. DE JONGH, W. J. CRAMA, AND D. J. W. IJDO, *Physica B* **83**, 97 (1976).
21. G. OLLIVIER, *Phys. Status Solidi A* **30**, 383 (1975).
22. A. ABRAGAM AND B. BLEANEY, "Electron Paramagnetic Resonance of Transition Ions," pp. 431, 399, Oxford Univ. Press, London (1970).
23. G. SPERLICH, K. H. JANNECK, AND K. H. J. BUSCHOW, *Phys. Status Solidi B* **57**, 701 (1973).
24. J. B. GOODENOUGH, *Phys. Rev.* **164**, 785 (1967).
25. N. YAMAMOTO, M. KIYAMS, AND T. TAKADA, *Japan. J. Appl. Phys.* **12**, 1827 (1973).
26. The angular dependence of the superexchange interaction is discussed by R. RITTER, L. JANSEN, AND E. LOMBARDI, *Phys. Rev. B* **8**, 2139 (1973).
27. G. S. RUSHBROOK AND P. J. WOOD, *Mol. Phys.* **1**, 257 (1958).
28. G. S. RUSHBROOK AND P. J. WOOD, *Mol. Phys.* **6**, 409 (1963).
29. L. J. DE JONGH, *AIP Conf. Proc.* **10**, 561 (1972).
30. A. H. MORRISH, "The Physical Principles of Magnetism," p. 447, Wiley, New York (1965).
31. M. J. HENNESSY, C. D. MCELVEE, AND P. M. RICHARDS, *Phys. Rev. B* **7**, 930 (1973).